Reaction Dynamics of β-Hydrogen Transfer in the Zirconocene Olefin Polymerization Catalyst: A DFT Path Sampling Study

Christopher N. Rowley and Tom K. Woo*

Centre for Catalysis Research and Innovation, Department of Chemistry, University of Ottawa, 10 Marie-Curie, Ottawa, Ontario K1N 6N5, Canada

Received September 13, 2008

Summary: The reaction dynamics of β-hydrogen transfer in the zirconocene olefin polymerization catalyst was modeled using DFT path sampling. Trajectories were found to cross the reaction barrier at a broad range and showed that Zr−H bonding increases during the reaction due to dynamic effects and a Zr−(η^2-C_2H_4) fluctuation is critical to inducing the transfer.

Since the advent of density functional theory (DFT), computer modeling has made significant contributions to the study of organometallic reaction mechanisms.[1] One limitation of conventional DFT mechanistic studies is that only the potential energy minima and transition states (TS) are characterized. Finite temperature effects arising from the dynamic behavior of these complexes, such as vibrational and fluxional effects,[2] are difficult to investigate thoroughly using these methods.

Molecular dynamics (MD) provides an elegant and direct means to examine finite temperature effects by simulating the motion of the atoms of a system through time. In combination with DFT, MD has made significant contributions to our understanding of both fundamental[3] and complex chemical systems,[4] including many notable examples in organometallic chemistry.[5] As this method is computationally demanding, the time scales that can be simulated are generally too short (<100 ps) to observe chemical reactions, unless artificial forces or constraints are imposed. However, when such biases are imposed on the MD simulation, the true dynamics of the system are masked. Transition path sampling is a novel Monte Carlo technique that overcomes this limitation by focusing an MD simulation on a reaction, efficiently generating an unbiased ensemble of short, reactive trajectories.[6] In recent years, path sampling has been used in several landmark studies of chemical reaction dynamics[7] and is emerging as a promising tool to study organometallic reaction mechanisms.[8]

Group 4 metallocene olefin polymerization catalysts have been the subject of intense study during the last 25 years and have served as a framework for the development of alternatives to heterogeneous Ziegler−Natta catalysts.[9] The length of the polymer chain produced by these catalysts is largely determined by the relative rates of chain propagation and chain termination. As polymer chain length has a major influence on the physical properties of the resultant material, there is significant interest in better understanding the chain termination processes. β-Hydrogen transfer from a growing polymer chain to a monomer has been identified as an important chain termination mechanism, wherein a hydrogen (denoted here as H_T) is transferred from C_β of the growing chain to a coordinated olefin monomer. There has been extensive computer modeling of this pathway,[10] as this reaction mechanism is of considerable academic and industrial importance. With the aim of gaining novel insights into this mechanism, we used path sampling to examine its reaction dynamics. We harvested 350 reactive trajectories of the degenerate transfer a β-hydrogen from an ethyl ligand to ethene in the cationic $Cp_2Zr(C_2H_5)(C_2H_4)$ complex, a popular model for chain transfer in the mainstay zirconocene olefin polymerization catalyst.

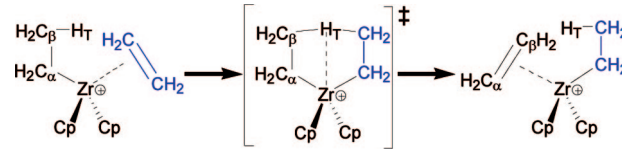

The established structural and bonding features of the β-hydrogen transfer are apparent in the reaction potential energy surface, using coordinates of the length of the C_β−H_T bond broken and the Zr−H_T distance (Figure 1). The long, elliptical reactant minimum is characteristic of a strong β-agostic interaction, which stabilizes configurations with short Zr−H_T distances

* To whom correspondence should be addressed. E-mail: twoo@uottawa.ca.

(1) (a) Niu, S. Q.; Hall, M. B. *Chem. Rev.* **2000**, 100. (b) Ziegler, T.; Autschbach, J. *Chem. Rev.* **2005**, *105*, 2695–2722.

(2) (a) Michalak, A.; Ziegler, T. *J. Phys. Chem. A* **2001**, *105*, 4333–4343. (b) Seth, M.; Senn, H. M.; Ziegler, T. *J. Phys. Chem. A* **2005**, *109*, 5136–5143.

(3) (a) Marx, D.; Tuckerman, M. E.; Hutter, J.; Parrinello, M. *Nature* **1999**, *397*, 601–604. (b) Raugei, S.; Klein, M. L. *J. Am. Chem. Soc.* **2001**, *123*, 9484–9485. (c) Kuo, I. F. W.; Mundy, C. J. *Science* **2004**, *303*, 658–660.

(4) (a) Reinhardt, S.; Marian, C. M.; Frank, I. *Angew. Chem., Int. Ed.* **2001**, *40*, 3683–3685. (b) Tse, J. S. *Annu. Rev. Phys. Chem.* **2002**, *53*, 249–290. (c) Minary, P.; Tuckerman, M. E. *J. Am. Chem. Soc.* **2005**, *127*, 1110–1111. (d) Mosey, N. J.; Mueser, M. H.; Woo, T. K. *Science* **2005**, *307*, 1612–1615.

(5) (a) Margl, P.; Lohrenz, J. C. W.; Woo, T. K.; Ziegler, T.; Blöchl, P. E. *Polym. Mater. Sci. Eng.* **1996**, *74*, 397–8. (b) Woo, T. K.; Margl, P. M.; Ziegler, T.; Bloechl, P. E. *Organometallics* **1997**, *16*, 3454–3468. (c) Margl, P. M.; Woo, T. K.; Bloechl, P. E.; Ziegler, T. *J. Am. Chem. Soc.* **1998**, *120*, 2174–2175. (d) Woo, T. K.; Margl, P. M.; Deng, L.; Cavallo, L.; Ziegler, T. *Catal. Today* **1999**, *50*, 479–500. (e) De Angelis, F.; Fantacci, S.; Sgamellotti, A. *Coord. Chem. Rev.* **2006**, *250*, 1497–1513. (f) Magistrato, A.; Togni, A.; Rothlisberger, U. *Organometallics* **2006**, *25*, 1151–1157. (g) Buhl, M.; Golubnychiy, V. *Organometallics* **2007**, *26*, 6213–6218. (h) Gossens, C.; Tavernelli, I.; Rothlisberger, U. *J. Am. Chem. Soc.* **2008**, *130*, 10921–10928.

(6) (a) Bolhuis, P. G.; Chandler, D.; Dellago, C.; Geissler, P. L. *Annu. Rev. Phys. Chem.* **2002**, *53*, 291–318. (b) Rowley, C. N.; Woo, T. K. *J. Chem. Phys.* **2007**, *126*, 024110/1–024110/8.

(7) (a) Geissler, P. L.; Dellago, C.; Chandler, D.; Hutter, J.; Parrinello, M. *Science* **2001**, *291*, 2121–2124. (b) van Erp, T. S.; Meijer, E. J. *Angew. Chem., Int. Ed.* **2004**, *43*, 1660–1662. (c) Basner, J. E.; Schwartz, S. D. *J. Am. Chem. Soc.* **2005**, *127*, 13822–13831.

(8) (a) Snee, P. T.; Shanoski, J.; Harris, C. B. *J. Am. Chem. Soc.* **2005**, *127*, 1286–1290. (b) Rowley, C. N.; Foucault, H. M.; Woo, T. K.; Fogg, D. E. *Organometallics* **2008**, *27*, 1661–1663. (c) Rowley, C. N.; Woo, T. K. *J. Am. Chem. Soc.* **2008**, *130*, 7218–7219. (d) Bergeron, D. E.; Coskuner, O.; Hudgens, J. W.; Gonzalez, C. A. *J. Phys. Chem. C* **2008**, *112*, 12808–12814.

10.1021/om800891w CCC: $40.75
Publication on Web 11/17/2008

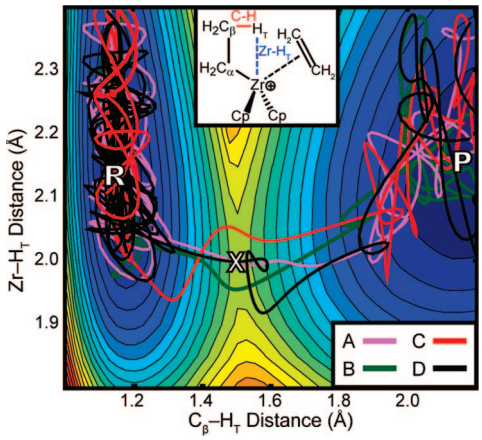

Figure 1. Potential energy surface of the β-hydrogen transfer reaction with selected trajectories plotted. R and P indicate the reactant and product potential energy minima, respectively, and X indicates the TS. Contours are at 0.83 kcal mol^{-1} intervals.

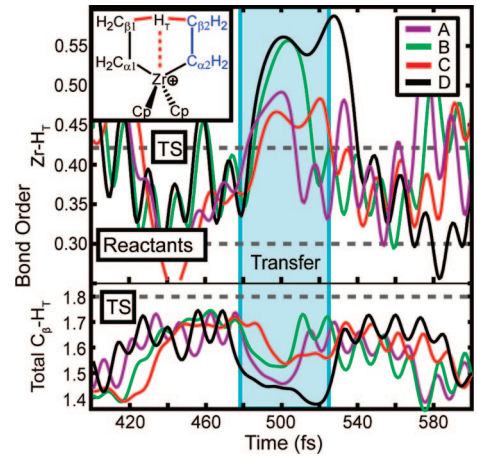

Figure 2. Zr−H$_T$ bond order and sum of C$_\beta$−H$_T$ bond orders during the transition event of trajectories **A**−**D**. Bond orders of potential energy TS and minimum are shown in gray.

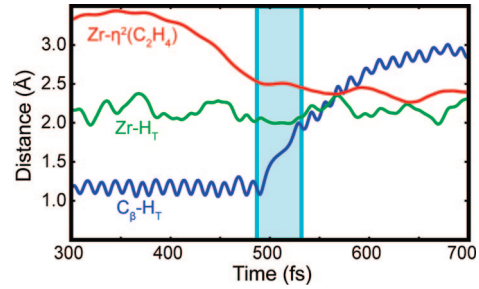

Figure 3. Structural fluctuations in trajectory **A** during the transfer.

and long C−H$_T$ bonds. A partial Zr−H$_T$ bond plays a critical role in the transfer. Although the Zr−H$_T$ interaction stabilizes the transition state to a greater degree at short Zr−H$_T$ distances, this is offset by increasing C−Zr−C bond angle strain when this distance is decreased further. Due to the close competition of these two effects, there is a broad TS region (1.95 Å < Zr−H$_T$ distance < 2.05 Å) where the energy is within 1 kcal mol^{-1} of the 9.7 kcal mol^{-1} TS, a feature first noted by Talarico and Budzelaar.[11]

Due to the broad TS, trajectories in the path ensemble are able to cross the barrier throughout the range of Zr−H$_T$ = 1.95−2.05 Å.[12] Although analysis of the path ensemble shows that the barrier crossing occurs quickly, with an average transition time of 38 ± 9 fs, the range is broad (20−63 fs) and the trajectories exhibit complicated reaction dynamics. We have selected four trajectories to illustrate the variety of transitions in the path ensemble: **A** crosses the barrier near the potential energy TS, **B** crosses the barrier low on the Zr−H$_T$ coordinate, **C** crosses the barrier high on the Zr−H$_T$ coordinate, and **D** shows an interesting partial recrossing.

To examine dynamic effects on the transfer reaction, we have calculated the Zr−H$_T$ Mayer bond orders in the four selected trajectories, as shown in Figure 2. **B** crosses the barrier closest to the metal and consequently experiences strong Zr−H$_T$ bonding, although **D** experiences even stronger bonding during its descent to the product minimum. Despite crossing considerably further from the metal, **C** experiences Zr−H$_T$ bonding comparable to **A**, which crosses near the TS. Interestingly, all four trajectories show Zr−H$_T$ bond orders that are notably greater than the bond order value from the transition state.[13] This indicates that the dynamic effects increase the role of Zr−H$_T$ bonding during the transfer. Another notable dynamic effect is observed with the sum of the two C$_\beta$−H$_T$ bond orders (C$_{\beta1}$−H$_T$ + C$_{\beta2}$−H$_T$). As shown in the lower part of Figure 2, this sum of bond orders for the dynamic trajectories is consistently below the value experienced at the potential energy TS.

These two effects can be quantified by comparing the bond orders of the static transition state to the bond orders of the step in the dynamic trajectories where H$_T$ is equidistant from C$_{\beta1}$ and C$_{\beta2}$. The average Zr−H$_T$ bond order at these "dynamic transition states" is 0.49 ± 0.02, indicating a systematically larger bond order than the static value of 0.43 with a significant range. Similarly, the average sum of C$_\beta$−H$_T$ bond orders is 1.53 ± 0.03, a fairly broad range that is significantly lower than the static transition state value of 1.8. These results can be interpreted by considering the dynamics of the hydrogen transfer. The fluctuation that breaks the C$_\beta$−H$_T$ bond results in a distortion away from the optimal TS geometry where C$_\beta$−H$_T$ bonding is maximized. The Zr bonding adjusts to compensate for this via the Zr−H$_T$ interaction, originating from persistent Zr(d$_{z^2}$)−H$_T$(1s) overlap.

The large fluctuations in Zr−H$_T$ bond orders prior to the transfer led us to analyze the geometric parameters of the reactive trajectories in order to identify the important molecular fluctuations involved this reaction (Figure 3). The C$_\beta$−H$_T$ bond broken in the reaction undergoes only modest oscillations prior to the reactive event. Similarly, although the Zr−H$_T$ distance

(9) (a) Brintzinger, H. H.; Fischer, D.; Muelhaupt, R.; Rieger, B.; Waymouth, R. M. *Angew. Chem., Int. Ed.* **1995**, *34*, 1143–1170. (b) Resconi, L.; Cavallo, L.; Fait, A.; Piemontesi, F. *Chem. Rev.* **2000**, *100*, 1253–1345.

(10) (a) Margl, P.; Deng, L.; Ziegler, T. *J. Am. Chem. Soc.* **1999**, *121*, 154–162. (b) Margl, P.; Lohrenz, J. C. W.; Ziegler, T.; Bloechl, P. E. *J. Am. Chem. Soc.* **1996**, *118*, 4434–4441. (c) Talarico, G.; Budzelaar, P. H. M. *J. Am. Chem. Soc.* **2006**, *128*, 4524–4525. (d) Talarico, G.; Budzelaar, P. H. M. *Polym. Prepr.* **2006**, *47*, 466. (e) Talarico, G.; Budzelaar, P. H. M. *Organometallics* **2008**, *27*, 4098–4107.

(11) Talarico and Budzelaar noted that this broad transition state is common among many olefin polymerization catalysts and results in a preference for a secondary hydrogen transfer transition state in some cases.[10c−e]

(12) A plot of the all trajectories on the PES is included in the Supporting Information.

(13) This is in addition to the normal fluctuations observed in the Zr−H$_T$ bond, at the reactant or product. It should also be noted that the Zr−H$_T$ bond order has a maximum value at the static transition state along the reaction's idealized IRC.

undergoes a fluctuation into the 2.0 Å range during the transfer, this fluctuation occurs a number of times in the simulation without inducing a reaction. The distance between the incoming ethene and the metal is more determinative; in each trajectory sampled, there is a sharp decrease in the $Zr-\eta^2(C_2H_4)$ distance prior to the insertion. This fluctuation, beginning 120 ± 27 fs prior to the reactive event, corresponds to the orientation of the incoming ethene close to the metal, where it can accept the β-hydrogen from the ethyl ligand.

Path sampling has allowed us to examine the reaction dynamics of the β-hydrogen transfer in the zirconocene olefin polymerization catalyst. The path ensemble shows that this reaction exhibits diverse and complex reaction dynamics due to the broad reaction barrier. Remarkably, in the dynamic trajectories, $Zr-H_T$ bonding became stronger and $C_\beta-H_T$ bonding became weaker during the transfer, suggesting that finite temperature effects in organometallic reactions can significantly affect metal bonding interactions. While $C_\beta-H_T$ and $Zr-H_T$ fluctuations are essential to the transfer, a decrease in the $Zr-\eta^2(C_2H_4)$ beginning on average 120 fs prior to the transfer appears to be the critical event to induce the reaction. We are currently using path sampling to examine finite temperature effects involving counterions and solvents in this and other organometallic reactions. In particular, the effect of finite temperature effects on metal−ligand binding during chemical reactions demands further investigation.

Acknowledgment. We thank the NSERC and the Canada Research Chairs program for funding and the NSERC and HPCVL for graduate scholarships (C.N.R.). We are also grateful to the CFI, the Ontario Research Fund, and IBM Canada for providing computing resources.

Supporting Information Available: Text, a figure, and tables giving details of the calculations and MPEG files giving animations of a representative trajectory. This material is available free of charge via the Internet at http://pubs.acs.org.

OM800891W